# Supporting Information
# for

Multiterminal Quantized Conductance in InSb Nanocrosses

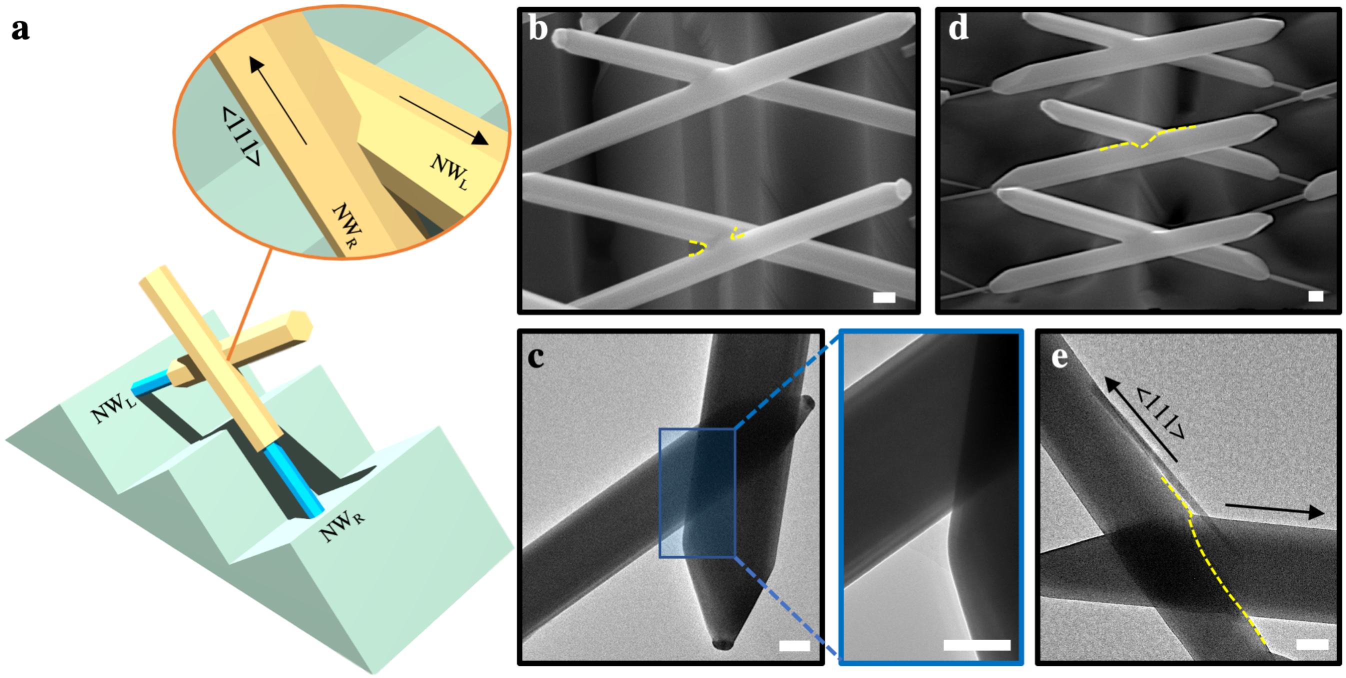


FIG. S1. **Structural analysis of partially intersected and marginally overlapped InSb nanocrosses.** **a**, Schematic of the opposite directional InSb NWs partially intersected through the sidewall due to radial growth. **b**, Tilted SEM image of InSb nanocrosses, where NWs are moderately meet (or overlap) each other through the facets when final InSb diameter is reached. **c**, TEM analysis of the similar nanocross, as shown in panel (**b**), where NWs are slightly touched but not intersected through each other. The magnified TEM image in the right confirms the overlapping, as no intersection is observed. **d**, Tilted SEM image of the nanocrosses, where NWs are marginally intersected from the sidewall after final growth time. **e**, TEM image of the similar nanocross. It is clearly observed that NWs are intersected to each other, unlike the previous one. Scale bars are 100 nm.

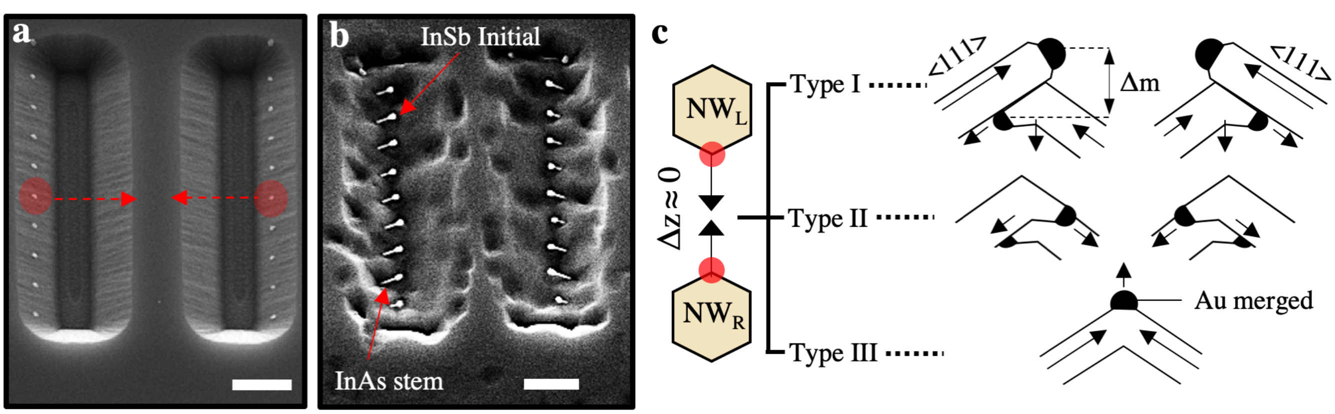


FIG. S2. **Head-to-head Au catalyst position** **a**, Tilted SEM image of the trenches, where the Au catalysts are lithographically positioned without any offset. **b**, Initial InSb section grown with InAs stem. **c**, Schematic of the three possible types of nanostructure formation when InSb NWs are grown head-to-head towards each other. Here, $\Delta m$ is the distance of the merging point from the Au catalyst. Scale bars for (**a**) and (**b**) are 1 $\mu$m.

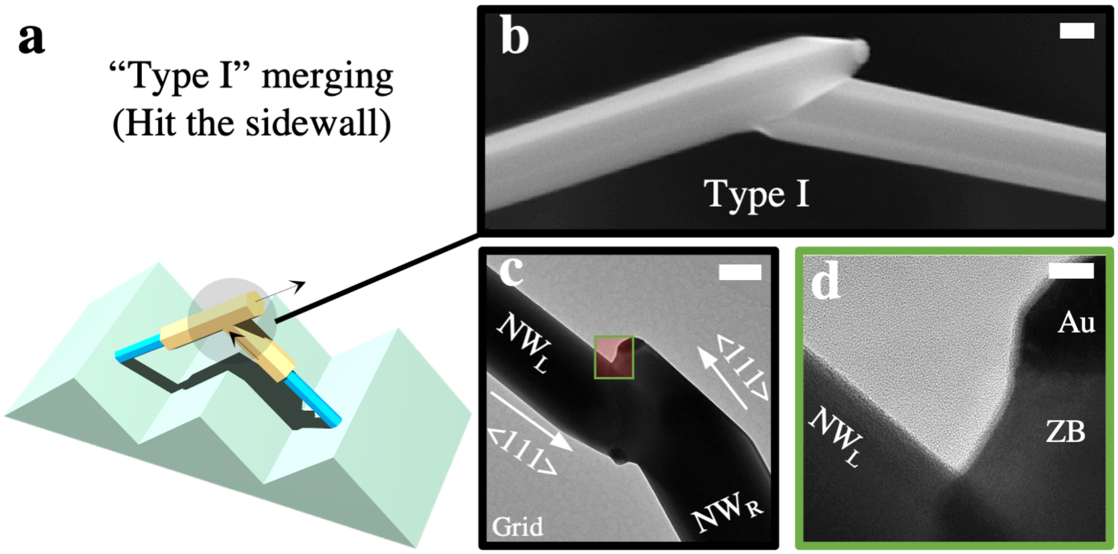


FIG. S3. **"Type I" merging.** **a**, Schematic of the "Type I" InSb network. Here, one NW hit on the side-wall of another NW with an offset. **b**, Tilted SEM image of the "Type I" merging. **c**, TEM analysis of the similar phenomena, where Au catalysts are well separated from each other after merging. **d**, Magnified highlighted section from panel (**c**). Scale bars for (**b**), (**c**), (**d**) are 100, 50 and 5 nm respectively.

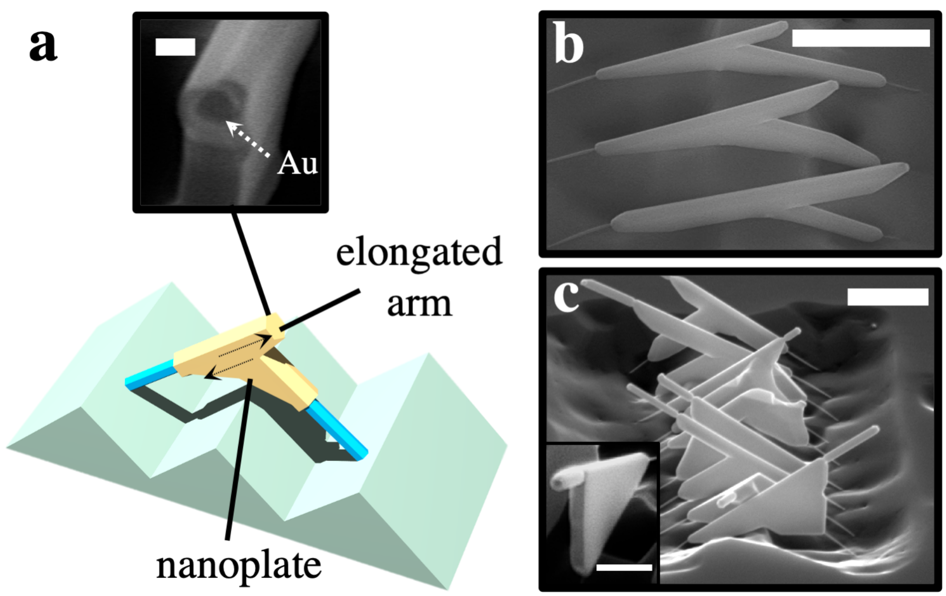


FIG. S4. **InSb nanoplate with elongated arm.** **a**, Schematic of the InSb nanoplate with a long arm. Inset SEM image demonstrates the top view of the elongated arm. **b**, Tilted SEM image, where all the arms are in the same direction. **c**, Tilted SEM image, where arms are shown two different directions demonstrating domination of kinetics of the Au catalyst to determine the direction of the arm. Inset is the top view demonstrating the triangular nanoplate section. Scale bar for (**a**) is 100 nm. Scale bars for (**b**) and (**c**) are 1 $\mu$m.

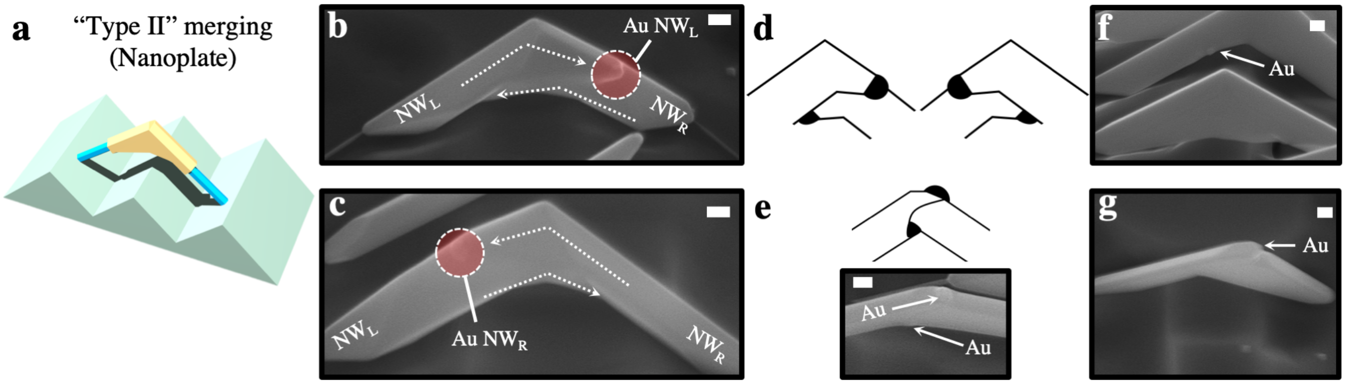


FIG. S5. **InSb network with "Type II" merging.** **a**, Schematic of the InSb network created after "Type II" merging. **b**, Tilted SEM image of InSb network where Au catalysts of $NW_L$ and $NW_R$ slide through each other facets after the meeting. The highlighted red circle shows the Au catalyst's position after the final growth time. **c**, SEM image shows the similar phenomena as (**b**), but in the opposite directions. **d**, Schematic of the Au position to create network shown in panel (**b**) and (**c**). **e**, Schematic and inset SEM shows the condition, where Au catalysts sit on the top and bottom facets of the NWs instead of side facets. **f**, Tilted SEM image of the nanoplate where upper NW slides on $(10\bar{1})$ and $(0\bar{1}\bar{1})$ facets and at the same time bottom NW crawl through $(011)$ and $(\bar{1}01)$ facets in opposite $< 111 >$ directions. **g**, Tilted SEM image of the nanoplate structure, where Au catalyst of $NW_L$ stays in the top facet, whereas the $NW_R$ catalyst crawl through the sidewall similar to other conditions.

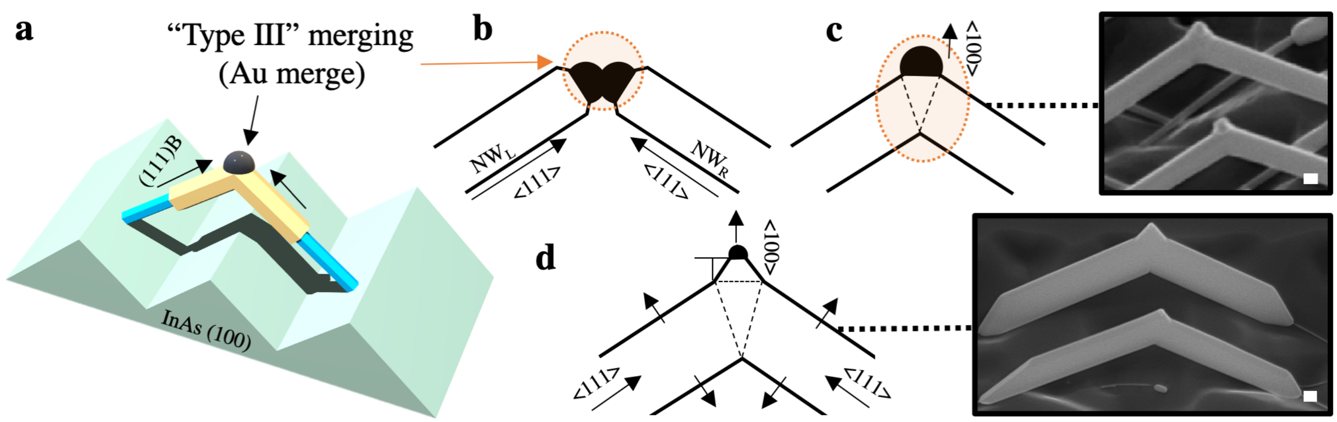


FIG. S6. **"Type III" merging with InSb network.** **a**, Schematic of the "Type III" merging. Here, $\Delta$y and $\Delta$m are zero, as a result, Au droplets of both NWs merge. **b**, Initial stage of the merging, where two Au droplets meet. **c**, Second stage of the merging, where Au droplets are combined into one. On the right, SEM image of such structure. **d**, In the last stage, Au droplet assists growing in $< 100 >$ direction for longer growth time. SEM image on the right shows similar results in long growth time. Scale bars for (**c**) and (**d**) are 100 nm.

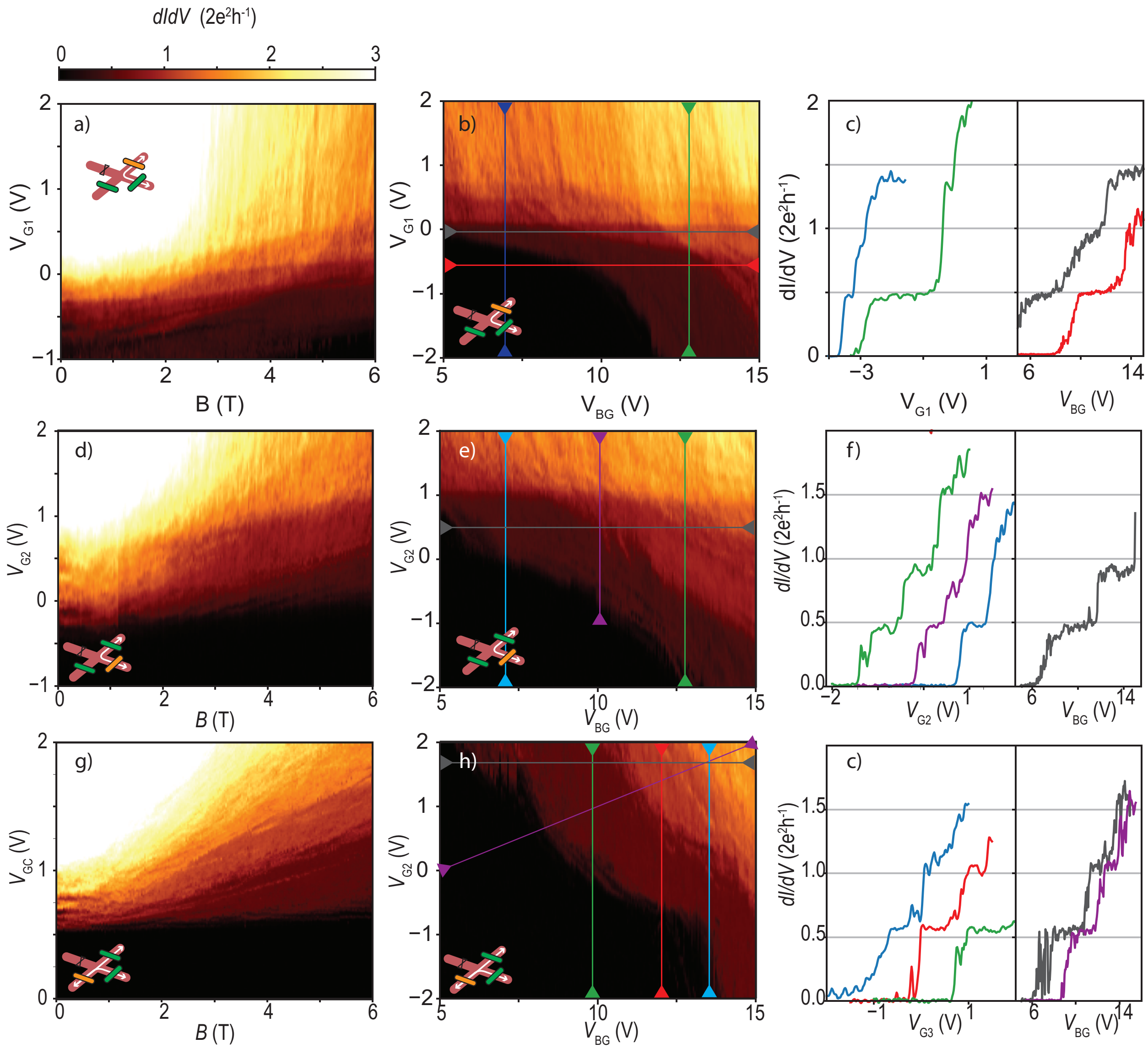

FIG. S7. **Full datasets of field and gate dependencies of individual quantum point contacts. a-b-c** is the analogous data-set for terminal 1, while the two QPCs in parallel are more visible the Zeeman splitting of the conductance plateaus is not as linear. **d-e-f** depicts terminal 2 as in the main text. **g-h-i** shows the behavior of terminal 3. Since this terminal has lower overall conductivity due to the nearby terminal 4 only the first plateau is accessible at a backgate voltage of +10V. Panel (**g**) is thus sweeping top and backgate together along the purple line to show the evolution of more than one plateau. For the first two rows we extract the conductance by taking the conductance between terminals 1 and 2 only, because terminal 3 is at a single conductance quantum and as such the transport is dominated by g12. For the conductance of terminal 3, we sum g13 and g23, as approximately half of the current flowing through terminal 3 flows into each of them.

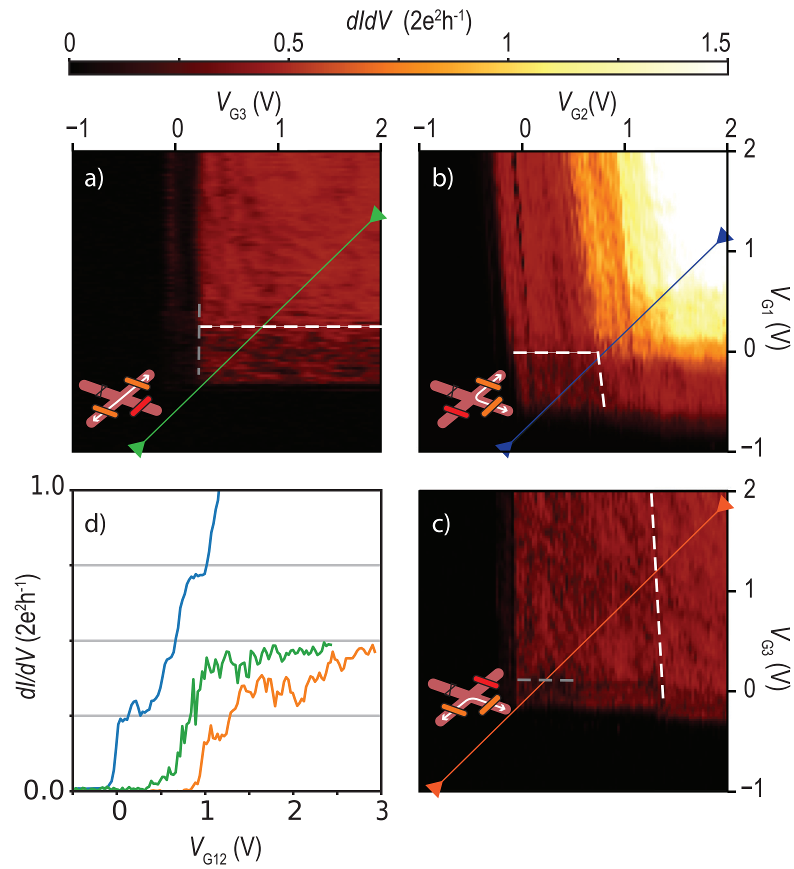


FIG. S8. **Full datasets of 2 QPCs in series. a-b-c** depicts two QPCs in series, panel (**b**) is the same dataset as in the main text. We note that because terminal 3 does not open to more than 1 conductance plateau, it is not possible to access the regime where both QPCs are open with multiple channels. All three datasets show a sum of conductance below $e^2/h$ for both QPCs at one conductance quantum, with all of them showing resonances on top of a $e^2/2h$ baseline. **d** shows the linecuts hinted in the colormaps without averaging.